Inorganic Chemistry

Communication

pubs.acs.org/IC

In Vitro and in Vivo Fluorescent Imaging of a Monofunctional Chelated Platinum Complex Excitable Using Visible Light

Shengde Wu,‡ Chengcheng Zhu,‡ Changli Zhang, Zhen Yu, Weijiang He,* Yafeng He, Yizhi Li, Jing Wang, and Zijian Guo*

State Key Laboratory of Coordination Chemistry, School of Chemistry and Chemical Engineering, Nanjing, 210017, People's Republic of China

Supporting Information

ABSTRACT: The biological fluorescent distribution of a model antitumor monofunctional platinum(II) complex bearing a 7-nitro-2,1,3-benzoxadiazole fluorophore can be visualized in breast carcinoma MCF-7 cells, pulmonary carcinoma A549 cells, kidney epithelial 293T cells, and zebrafish larva.

Although atom-based techniques such as X-ray fluorescence are able to map the cellular distribution of an antitumor platinum(II) complex,[1] molecular fluorescence imaging displays the advantage in visualizing in situ the cellular platinum(II) uptake, distribution, and transportation. In fact, the intracellular temporal/spatial platinum(II) information offered by this noninvasive technique is especially appealing to understanding the mechanism of action and side effects of current platinum-(II)-based anticancer drugs.[2,3] Therefore, attempts have been made to tether fluorophore to platinum(II) complexes to clarify their intracellular distribution.[4,5] However, in vivo fluorescence platinum(II) imaging in a live animal model, which is helpful to clarifying the actual platinum(II) transportation and distribution in tissues and organs of the live body, has not been reported so far. This requires fluorescent platinum(II) complexes of longer excitation wavelength to enhance the imaging depth and reduce the UV-induced cell damage/autofluorescence interference. Because the low stability of a normal near-infrared (NIR) fluorophore limit its suitability to be tethered to platinum(II)-based anticancer drugs, the more stable visible-light-excited platinum(II) complexes become attractive choices for in vivo platinum(II) imaging of small transparent animal models like zebrafish. Cisplatin-derivatived fluorescent probes of visible-light excitability such as CFDA-Pt, FDDP, and Alexa-Fluor 546−cisplatin have been reported to explore the intracellular distribution of cisplatin,[4a,6] while the cyclometalated platinum(II) complexes were reported as dyes for cell imaging because of their photostability and long luminescence lifetime.[7]

We have reported a series of monofunctional anticancer platinum(II) complexes with pyridine/quinoline derivatives as the ligands.[8] Many of them display anticancer spectra different from that of cisplatin. They show also the advantage over the anticancer polynuclear platinum(II) complex BBR3464 for its framework integrality in the presence of glutathione (GSH) owing to the tridentate chelating effect.[8a,9] These complexes possess the chelated Pt^{II} centers of one positive charge and one leaving group. Herein, a new fluorescent platinum(II) complex, [Pt**L**Cl]Cl, was constructed by tethering a tridentate chelating Pt^{II} center, Pt(BPA) motif [BPA = *N*,*N*-bis(pyridin-2-ylmethyl)amine], to a fluorophore 4-amino-7-nitro-2,1,3-benzoxadiazole (4-amino-NBD) to explore the in vitro/in vivo processing and distribution of monofunctional chelated platinum(II) complexes. The visible-light excitability and biocompatibility of an NBD fluorophore should favor the related cell imaging to clarify the specific antitumor activity of monofuctional chelated platinum(II) complexes.[10]

The ligand **L** and its platinum(II) complex [Pt**L**Cl]Cl were prepared by modified procedures.[8a] A single crystal of [Pt**L**Cl]Cl·H_2O was obtained by evaporation of its aqueous methanol solution in the dark. Structure resolution by X-ray diffraction demonstrates that this complex crystallizes in a $P\bar{1}$ space group. The Pt^{II} center is coordinated by three N atoms of BPA and one Cl^- ion in a square-planar geometry (Figure 1b and Tables S1 and S2 in the Supporting Information, SI). An ^1H NMR study in dimethyl sulfoxide (DMSO)-d^6 found that platinum(II) coordination makes the singlet at 3.89 ppm for 2-pyridylmethylene protons become two doublets at 4.98 and 5.40 ppm (Figure S2 in the SI), implying that the two methylene protons become diastereotopic and no longer equivalent. The fluorescence spectrum of **L** in a phosphate-buffered saline (PBS) buffer exhibits weak fluorescence with emission and excitation maxima at 546 and 467 nm, respectively (Figure 1c). Platinum(II) coordination of **L** leads to a 5-fold emission enhancement without any distinct shift in emission, and the mass spectrometry (MS) determination demonstrates the signal of $[Pt\mathbf{L}Cl]^+$. Although **L** was reported as a Zn^{2+} sensor,[11] the presence of 10 equiv of Zn^{2+} does not induce any obvious change in the fluorescence (Figure S3 in the SI) and MS spectra of [Pt**L**Cl]Cl in ambient conditions. In addition, [Pt**L**Cl]Cl shows lower cytotoxicity to the human pulmonary carcinoma cell (A549), breast carcinoma (MCF-7), and ovarian cancer cell lines (COC1 and CAOV3) compared with cisplatin. Its IC_{50} value against MCF-7 cells is 45.9 μM, which is 3.4-fold higher than that of cisplatin (48 h, MTT; Table S3 in the SI). However, lower cytotoxicity affords longer cell survival time for cell imaging.

Confocal imaging of MCF-7 cells demonstrated a punctuated distribution pattern in cytoplasm after 20 min of **L** incubation. The costaining imaging with Hoechst 33342 confirmed that **L**

Received: July 14, 2011
Published: October 28, 2011

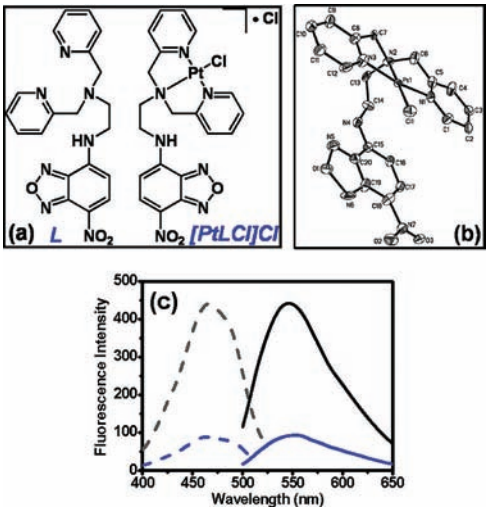

Figure 1. (a) Compound **L** and [Pt**L**Cl]Cl. (b) Thermal ellipsoid plot (30% probability) of [Pt**L**Cl]Cl·H_2O. Protons, non-coordinating Cl atom, and water molecules were omitted for clarity. (c) Excitation (---) and emission spectra (—) of [Pt**L**Cl]Cl (black, 0.01 mM) and **L** (blue, 0.01 mM) in a PBS buffer containing 0.3% DMSO.

could not enter into the nucleus (Figure S4 in the SI). Upon incubation with [Pt**L**Cl]Cl, the cells show bright peripheric dotted lines on the cell membrane in the initial 150 min (Figure

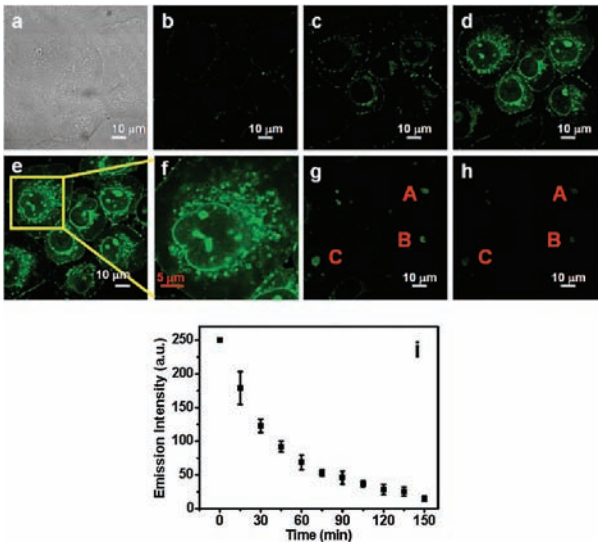

Figure 2. Confocal fluorescence imaging of MCF-7 cells incubated with [Pt**L**Cl]Cl (10 μM) at 25 °C (λ_{ex}, 488 nm; band path, 550−600 nm): (a) bright-field image; fluorescence image after 0.5 h (b), 3 h (c), 4 h (d), and 5 h (e); (f) zoom of pane e. After 6 h of incubation, the cells in pane e were incubated with 1× PBS buffer and images were obtained after 15 min (g) and 60 min (h). (i) Emission profile according to spots A−C in pane g.

2). After 3 h of incubation, more small bright vesicles and spots appear especially around the dim nucleus (Figure 2c). Bright spots appear in the nucleus in the later incubation procedure, suggesting that the complex can stride into the nucleus. After 4−5 h of incubation, many bright vacuoles were observed inside the cells and the cells became swollen, which is a common appearance for cell paraptosis (Figure 2f).[11] Replacing the platinum(II) solution with a PBS buffer after 6 h of incubation leads to the quick disppearance of cytoplasmic fluorescence in 15 min, while intranuclear fluorescence decreases slowly and attains equilibrium in ∼2 h (Figure 2i). This result suggests the higher binding ability of [Pt**L**Cl]Cl in the nucleus than in the cytoplasm. Although imaging on A549 and healthy kidney epithelial 293T cells displayed cell uptake, distribution, and process behavior similar to those on MCF-7 cells (Figures S5 and S6 in the SI), the cell uptake process by A549 cells is much slower, which might be related to the higher IC_{50} value of [Pt**L**Cl]Cl (99.4 μM) against A549 cells (Table S3 in the SI).[12]

After the complete disappearance of intracellular fluorescence induced by media replacement, the MCF-7 cells were stained with nucleolus dye SYTO 81,[13] and the observed bright spots are exactly colocalized with the intranuclear bright spots induced by [Pt**L**Cl]Cl incubation (Figure 3). The result implies

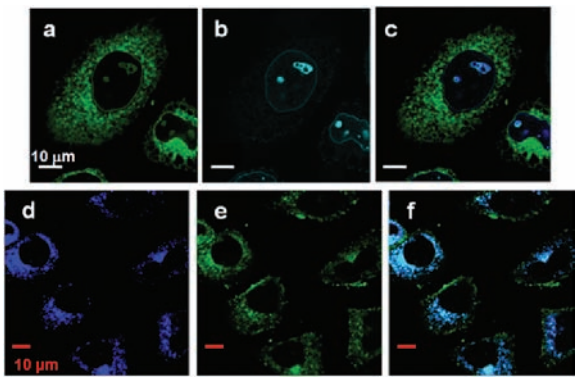

Figure 3. Confocal fluorescence images of MCF-7 cells: (a) cells after incubation with 10 μM [Pt**L**Cl]Cl at 25 °C for 6 h (λ_{ex}, 488 nm; band path, 550−600 nm); (b) cells in part a undergoing complete fluorescence disappearance via 1 h of PBS incubation, followed by SYTO 81 staining (1.0 μM, λ_{ex}, 514 nm; band path, 520−570 nm); (c) overlay of parts a and b; image of cells costained by Mito-tracker NC-M7514 and [Pt**L**Cl]Cl obtained via band path from 500 to 550 nm (d) and via band path from 550 to 600 nm (e) upon excitation at 488 nm; (f) overlay of parts d and e. Image d was obtained before [Pt**L**Cl]Cl incubation, and the imaging conditions were adjusted to make band path 550−600 nm display no fluorescence signal. Image e was obtained at the same condition after [Pt**L**Cl]Cl incubation.

the intensive affinity of [Pt**L**Cl]Cl to nucleic acids or related proteins in nucleolus. In fact, the circular dichroism spectrum of CT-DNA shows the distinct reduction of both positive and negative bands upon the addition of [Pt**L**Cl]Cl, while the addition of **L** leads to the intact spectrum (Figure S7 in the SI). The result implies that the Pt^{II} center in the complex induces effective DNA binding. In the meantime, DNA binding does not induce an obvious change in the emission spectrum of [Pt**L**Cl]Cl, indicating that DNA binding does not affect the emission of [Pt**L**Cl]Cl. Given the dim nucleus in the **L**-stained cells, the intranuclear fluorescence upon [Pt**L**Cl]Cl incubation suggests that the nucleus affinity of this complex is due to its Pt^{II} center. However, the protein in the nucleolus might also be involved in the binding.

The preferential affinity to mitochondria of this complex before entering into the nucleus has been confirmed by the colocalization pattern (overlap coefficient, 0.93) upon costaining with Mito-tracker NC-M7514 on MCF-7 cells (Figure 3d−f). This phenomenon is different from that of conventional fluorescent-tagged cisplatin analogues, which are neutral and

dx.doi.org/10.1021/ic201506y | Inorg. Chem. 2011, 50, 11847−11849

sequestered in lysosomes or other organelles.[4a,14] Moreover, the vacuole formation in the later incubation via the mitochondria swelling was visualized by fluorescence imaging (Figure S12 in the SI). This result implies that the cytotoxicity of this complex to MCF-7 cell lines might come from cell paraptosis, which is different from apoptosis induced by cisplatin.[15]

Compared with the fluorescence throughout the cells after 30 min of CFDA-Pt incubation,[4a] the slow enhancement of intracellular fluorescence in our case suggests that the cell uptake of the chelated monofunctional platinum(II) complex is much slower than that of the cisplatin analogues bearing no charge. Because **L** displays a quick uptake process, it is clear that the Pt^{II} center of [Pt**L**Cl]Cl reduces the uptake process. The aforementioned quick drop of cytoplasmic fluorescence indicates that the secretion of this complex is rapid. Although GSH triggers the emission drop of [Pt**L**Cl]Cl, its much slower drop rate suggests that a quick decrease of cytoplasmic fluorescence might be ascribed to the cellular efflux of [Pt**L**Cl]Cl. The efficient efflux might be a factor responsible for the lower cytotoxicity of [Pt**L**Cl]Cl against MCF-7 than cisplatin.

As a frequently used transparent small animal model, zebrafish larva should be suitable for construction of the in vivo platinum(II) imaging model, with the aid of complex [Pt**L**Cl]Cl of visible-light excitability and intracellular platinum(II) imaging ability. Without [Pt**L**Cl]Cl incubation, the larva display no clear bright region in the fluorescence image. However, the distinct bright fluorescence can be observed only on the liver of larva after 4 h of incubation with 50 μM [Pt**L**Cl]Cl (Figure 4). Moreover, the in vivo distribution pattern of this

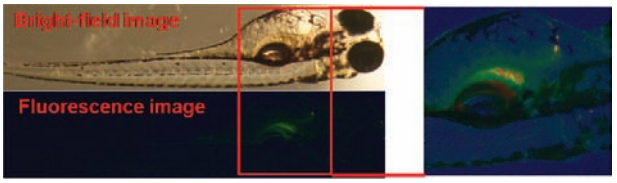

Figure 4. Images of 50 h-zebrafish larva recorded by a fluorescence stereomicroscope after 4 h of incubation with [Pt**L**Cl]Cl (50 μM). Right: zoom of the overlay of images in the red box.

platinum(II) complex in the larva is alterable because of the variable complex concentration and incubation time, and the long-term tracking at different concentrations is still undergoing.

In summary, the in vitro and in vivo fluorescence imaging of the 3N chelated monofunctional platinum(II) complex has been realized with the newly prepared NBD-tethered platinum(II) complex. Besides the slow cell uptake process and nucleolus affinity, this positively charged monofunctional platinum(II) complex displays preferential affinity to mitochondria. The current in vivo platinum(II) imaging demonstrates a reliable mode for in situ platinum(II) tracking in real time, which should promote understanding of the antitumor activity of platinum(II) complexes, favoring the development of platinum(II)-based antitumor drugs.

■ ASSOCIATED CONTENT

Supporting Information

X-ray crystallographic data in CIF format, synthetic procedures and characterization of **L** and [Pt**L**Cl]Cl, and other experimental details. This material is available free of charge via the Internet at http://pubs.acs.org.

■ AUTHOR INFORMATION

Corresponding Author

*Tel: +862583686218 (Z.G.), +862583597066 (W.H.). Fax: +862583314502. E-mail: heweij69@nju.edu.cn (W.H.), zguo@nju.edu.cn (Z.G.).

Author Contributions

‡Both authors contributed equally to this work.

■ ACKNOWLEDGMENTS

We thank the National Basic Research Program of China (Grant 2011CB935800), and the National Science Foundation of China (Grants 20871066, 10979019, and 21021062) for financial support.

■ REFERENCES

(1) (a) Shimura, M.; Saito, A.; Matsuyama, S.; Sakuma, T.; Terui, Y.; Ueno, K.; Yumoto, H.; Yamauchi, K.; Yamamura, K.; Mimura, H.; Sano, Y.; Yabashi, M.; Tamasaku, K.; Nishio, K.; Nishino, Y.; Endo, K.; Hatake, K.; Mori, Y.; Ishizaka, Y.; Ishikawa, T. *Cancer Res.* **2005**, *65*, 4998−5002. (b) Hall, M. D.; Foran, G. J.; Zhang, M.; Beale, P. J.; Hambley, T. W. *J. Am. Chem. Soc.* **2003**, *125*, 7524−7525.

(2) Wang, D.; Lippard, S. J. *Nat. Rev. Drug Discovery* **2005**, *4*, 307−320.

(3) (a) Klein, A. V.; Hambley, T. W. *Chem. Rev.* **2009**, *109*, 4911−4920. (b) Puckett, C. A.; Ernst, R. J.; Barton, J. K. *Dalton Trans.* **2010**, 1159−1170.

(4) (a) Molenaar, C.; Teuben, J.; Heetebrij, R. J.; Tanke, H. J.; Reedijk, J. *J. Biol. Inorg. Chem.* **2000**, *5*, 655−665. (b) New, E. J.; Duan, R.; Zhang, J. Z.; Hambley, T. W. *Dalton Trans.* **2009**, 3092−3101.

(5) Marqués-Gallego, P.; Dulk, H. D.; Brouwer, J.; Tanase, S.; Mutikainen, I.; Turpeinen, U.; Reedijk, J. *Biochem. Pharmacol.* **2009**, *78*, 365−373.

(6) (a) Safaei, R.; Katano, K.; Larson, B. J.; Samimi, G.; Holzer, A. K.; Naerdemann, W.; Tomioka, M.; Goodman, M.; Howell, S. B. *Clin. Cancer Res.* **2005**, *11*, 756−767. (b) Liang, X.-J.; Shen, D.-W.; Chen, K. G.; Wincovitch, S. M.; Garfield, S. H.; Gottesman, M. M. *J. Cell. Physiol.* **2005**, *202*, 635−641.

(7) (a) Botchway, S. W.; Charnley, M.; Haycock, J. W.; parker, A. W.; Rochester, D. L.; Weinstein, J. A.; Williams, J. A. G. *Proc. Natl. Acad. Sci. U.S.A.* **2008**, *105*, 16071. (b) Wu, P.; Wong, E. L. M.; Ma., D. L.; Tong, G. S. M.; Ng, K. M.; Che, C. M. *Chem.—Eur. J.* **2009**, *15*, 3652.

(8) (a) Zhao, Y.; He, W.; Shi, P.; Zhu, J.; Qju, L.; Lin, L.; Guo, Z. *Dalton Trans.* **2006**, 2617−2619. (b) Zhang, J.; Wang, X.; Tu, C.; Lin, J.; Ding, J.; Lin, L.; Wang, Z.; He, C.; Yan, C.; You, X.; Guo, Z. *J. Med. Chem.* **2003**, *46*, 3502−3507.

(9) Oehlsen, M. E.; Qu, Y.; Farrell, N. *Inorg. Chem.* **2003**, *42*, 5498−5506.

(10) Qian, F.; Zhang, C.; Zhang, Y.; He, W.; Gao, X.; Hu, P.; Guo, Z. *J. Am. Chem. Soc.* **2009**, *131*, 1460−1468.

(11) Jiang, W.; Fu, Q.-Q.; Fan, H.-Y.; Wang, W. *Chem. Commun.* **2008**, 259−260.

(12) (a) Tardito, S.; Isella, C.; Medico, E.; Marchio, L.; Bevilacqua, E.; Hatzoglou, M.; Bussolati, O.; Franchi-gazzola, R. *J. Biol. Chem.* **2009**, *284*, 24306−24319. (b) Sperandio, S.; Belle, I. D.; Bredesen, D. E. *Proc. Natl. Acad. Sci. U.S.A.* **2000**, *97*, 14376−14381.

(13) New, E. J.; Parker, D. *Org. Biomol. Chem.* **2009**, *7*, 851−855.

(14) Wlodkowic, D.; Skommer, J.; Darzynkiewicz, Z. *Cytometry, Part A* **2008**, *73A*, 496−507.

(15) Jung, Y.; Lippard, S. J. *Chem. Rev.* **2007**, *107*, 1387−1407.